

Determination of plastic hinge properties for static nonlinear analysis of FRP-strengthened circular columns in bridges

Gholamreza Ghodrati Amiri*¹, Azadeh Jaber Jahromi² and Benjamin Mohebi³

¹Center of Excellence for Fundamental Studies in Structural Engineering, School of Civil Engineering, Iran University of Science & Technology, Tehran, Iran

²School of Civil Engineering, Iran University of Science & Technology, Tehran, Iran

³Department of Civil engineering, Faculty of Engineering, Imam Khomeini International University, Qazvin, Iran

(Received July 7, 2010, Revised May 8, 2011, Accepted November 23, 2011)

Abstract. In the recent years, rehabilitation of structures, strengthening and increasing the ductility of them under seismic loads have become so vital that many studies has been carried out on the retrofit of steel and concrete members so far. Bridge piers are very important members concerning rehabilitation, in which the plastic hinging zone is very vulnerable. Pier is usually confined by special stirrups predicted in the design procedure; moreover, fiber-reinforced polymers (FRP) jackets are used after construction to confine the pier. FRP wrapping of the piers is one of the most effective ways of increasing moment and ductility capacity of them, which has a growing application due to its relative advantages. In many earthquake-resistant bridges, reinforced concrete columns have a major defect which could be retrofitted in different ways like using FRP. After rehabilitation, it is important to check the strengthening adequacy by dynamic nonlinear analysis and precise modeling of material properties. If the plastic hinge properties are simplified for the strengthened members, as the simplified properties which FEMA 356 proposes for non-strengthened members, static nonlinear analysis could be performed more easily. Current paper involves this matter and it is intended to determine the plastic hinge properties for static nonlinear analysis of the FRP-strengthened circular columns.

Keywords: plastic hinge; pushover analysis; finite element model; FRP; Ansys.

1. Introduction

Occurred earthquake in 1990s were very destructive to structures, especially old-code-designed ones. Besides, observed vulnerability in concrete structures urged repair and rehabilitation of them. Reinforced concrete bridges were also affected as girders, connections and especially piers of them were damaged. Poor transverse reinforcing and lap splices with small development length, particularly in plastic hinging zones, caused the piers to collapse under smaller loads. Hence, rehabilitation of the bridge piers became an important issue.

There are many reinforced concrete bridges in Iran and the world, constructed a few decades ago and damaged by fatigue, corrosion and natural disasters (like earthquake and storms) up to now. Because of high importance of such structures and also multiplicity of them, it is not usually

* Corresponding author, Professor, E-mail: ghodrati@iust.ac.ir

economical and feasible to replace them with new structures, while rehabilitation of them saves a large amount of time and money.

In the recent decades, some alternatives have been proposed to increase the moment and ductility capacity of piers, especially in plastic hinging zones. A very effective alternative is confinement of concrete, which increases ultimate strain, compressive strength and energy absorbing capacity. Furthermore, confinement of concrete columns, particularly in the conjunctions, improves the ductility of the member and the whole structure. Close application of transverse rebars has been always a way to confine the member, but now FRP composites are also used to confine concrete and increase its ductility.

Multiaxial compressive stress increases strength and ductility of the concrete as it prevents cracks from growing. Multiaxial stress could be produced by transverse rebar, steel plates or composites (FHWA 1995).

Application of steel jackets for confining concrete is with some difficulties. Steel, as an isotropic material, can not be wrapped around the column easily and it is complicated to optimize its strength under axial and radial loads. Moreover, because of high elasticity module of steel, the jacket carries a large amount of axial load which leads to its early buckling. Also, larger Poisson ratio of steel compared to concrete causes separation of the two materials and a delay in the activation of confinement (Vistaps and Karbhari 2004).

Contrary to other rehabilitation materials, FRP jacket has relatively more advantages like light weight, corrosion resistance, high flexibility and tensile strength, easy transportation and application, etc. Also, it is possible to strengthen FRP jackets externally. These advantages are the reasons for widespread use of FRP jackets in the construction industry today (FHWA 1995).

The industrial types of FRP are carbon FRP (CFRP), glass FRP (GFRP) and aramid FRP (AFRP), among which CFRP, though the high demand for it, is the most expensive one. Carbon fibers have high tensile strength and show a good resistance against fatigue and corrosion. They are also light and flexible with a small thermal expansion coefficient. As a disadvantage, CFRP is brittle in the failure and the corresponding strain is small. The other defects include the electrical conductivity and the high price of this type.

Glass FRP is the most common FRP in the industry due to its moderate cost and there are many types of GFRP concerning the mixed materials of it. The advantages of GFRP include: light weight, rather high tensile strength, good flexibility, easy transportation, fast and simple jacketing, high chemical resistance, thermal and electrical insulating property, sensitivity to abrasion and lower price compared to CFRP. GFRP jackets could be easily cut and they are also strengthened without destruction (ACI 440 2000).

Aramid FRP is famous for its high melting point, thermal resistance and insolubility in organic solvents. Production and application of AFRP is not as widespread as CFRP and GFRP due to its high cost. The most important properties of AFRP are light weight, high strength, fatigue resistance, insensitivity to cracks and insolubility in organic solvents, fuels and softeners; it is also possible to use AFRP up to 180 degrees Celsius.

In the past years, many studies have been carried out about confinement of the piers, increasing their strength and ductility and many reports on this subject are available too. Hence, offered behavior models for FRP-confined concrete columns are developing every day. For example, a part of ACI-2004 concerns the design of structures with FRP and its relationships (ACI 440 2000).

One of the rehabilitation methods for increasing moment and ductility capacity in structures (especially piers) is confinement with FRP jackets. Adequacy of rehabilitation with FRP is examined through

dynamic nonlinear analysis which is complicated to some extent. Hence, static nonlinear analysis (or pushover analysis) is performed which needs plastic hinge properties for these kinds of columns.

In this study, fifteen bridge piers are modeled by Ansys and lateral cyclic load is applied to them. Then the envelope curve is drawn for moment versus rotation hysteresis plots. Finally the required parameters for static nonlinear analysis are obtained.

2. History of previous works and theoretical background

2.1 History of stress - strain models of confined concrete

Multiaxial stress upgrades both strength and ductility of the concrete section, which is because of preventing cracks from growing. As already stated, multiaxial stress may be provided via concrete confinement by transverse reinforcement, steel plates or composites.

Early researches show that axial strength and strain, corresponding to active pressure of hydrostatic fluid, is calculated through the equation below in the confined concrete (Mander and Priestley 1988)

$$f'_{cc} = f'_{co} + k_1 f_1 \quad (1)$$

$$\varepsilon_{cc} = \varepsilon_{co} \left(1 + k_2 \frac{f_1}{f'_{co}} \right) \quad (2)$$

Where f'_{cc} and ε_{cc} are confined concrete strength and the corresponding strain under fluid lateral pressure or f_1 ; f'_{co} and ε_{co} are confined concrete strength and the corresponding strain; and k_1 and k_2 are coefficients which depends on the concrete mixture and lateral pressure (Mander and Priestley 1988).

Richart *et al.* (1928) found that average values of the coefficients for their tests is $k_1=4.1$ and $k_2=5$. In 1929, they also observed the same results of active pressure for confinement of the concrete section by close circular stirrups. Estimated value by Cosidere (1906) was $k_1=4.8$ and Balmer (1949) suggested a range of 4.5 to 7 for it with the mean value of 6.5 (Mander and Priestley 1988).

Stress-strain model by Kent and Park (1971) consists of a parabola (for increasing part) and a straight line (for decreasing part). In this model, confinement affects the slope of decreasing part (Hoshikuma *et al.* 1997). Newman *et al.* (1972) proved that k_1 depends on the confinement pressure so that it is not constant (Mander and Priestley 1988).

At the end of 1970s, primary efforts were made to confine concrete sections by nonmetal membranes. In 1978, Kurt employed PVC tube for casting concrete in it. The results showed a little upgrade of concrete strength due to the confinement, but plastics were not enough strength themselves. From that time forth, many other attempts were made to confine concrete sections (Saafi *et al.* 1999).

The first idea of confinement by composites was proposed by Fardis and Khalili (1982). They tested specimens confined by fiberglass and offered a stress-strain model on the basis of the model by Richart. Fardis and Khalili suggested a hyperbolic function to model stress-strain curve based on the data resulted from testing cylindrical concrete specimen wrapped by bidirectional FRP jacket (Samaan *et al.* 1998).

For many years, steel was the only material to confine the concrete. Hence, its confinement effects on the concrete had been studied widely. In 1988, Mander *et al.* (1988) offered a relationship for the confinement by steel which is the base of many stress-strain models of composite-confined

concrete. Their model could be applied to both circular and rectangular sections under static or dynamic (either uniform or cyclic) loads and it is adaptive to any confinement by steel (Mander and Priestley 1988).

As mentioned above, the model by Mander *et al.* (1988) is valid for circular and rectangular sections. In the current study, specimens have circular sections and Mander's model is employed. According to the model, compressive axial stress is obtained by

$$f_c = \frac{f'_{co} x r}{r - 1 + x'} \quad (3)$$

With

$$x = \frac{\varepsilon_c}{\varepsilon_{cc}} \quad (4)$$

$$\varepsilon_{cc} = \varepsilon_{co} \left[1 + 5 \left(\frac{f'_{cc}}{f'_{co}} - 1 \right) \right] \quad (5)$$

$$r = \frac{E_c}{E_c - E_{sec}} \quad (6)$$

$$E_{sec} = \frac{f'_{cc}}{\varepsilon_{co}} \quad (7)$$

where f'_{co} and ε_{co} are compressive strength and the corresponding strain of the unconfined concrete; E_c is elasticity module of it; and f'_{cc} and ε_{cc} are peak confined concrete stress and the corresponding strain. f'_{cc} is calculated as below

$$f'_{cc} = f'_{co} \left(-1.254 + 2.254 \sqrt{1 + \frac{7.94 f'_1}{f'_{co}}} - 2 \frac{f'_1}{f'_{co}} \right) \quad (8)$$

Effective lateral confining pressure or f'_1 is obtained through the relationship below

$$f'_1 = \frac{1}{2} k_e \rho_s f_{yh} \quad (9)$$

With

$$\rho_s = \frac{4 A_{sp}}{d_s \cdot s} \quad (10)$$

$$k_e = \frac{\left(1 - \frac{s}{2 d_s} \right)^2}{1 - \rho_{cc}} \quad (11)$$

Where ρ_s is volumetric ratio of stirrups of core concrete; A_{sp} is stirrup area; s is stirrup spacing; d_s is concrete core's diameter; f_{yh} is stirrup yield stress and ρ_{cc} is areal ratio of the longitudinal reinforcement to core concrete.

To determine the stress-strain curve of the cover concrete, it is assumed that the decreasing part, where $\varepsilon_c > 2\varepsilon_{co}$, is a straight line in which stress tends to zero in spalling strain or ε_{sp} .

In 1995, Nanni and Bradford studied the behavior of confined concrete wrapped in three types of FRP. They found that the model of Fardis and Khalili underestimates the ultimate strain considerably.

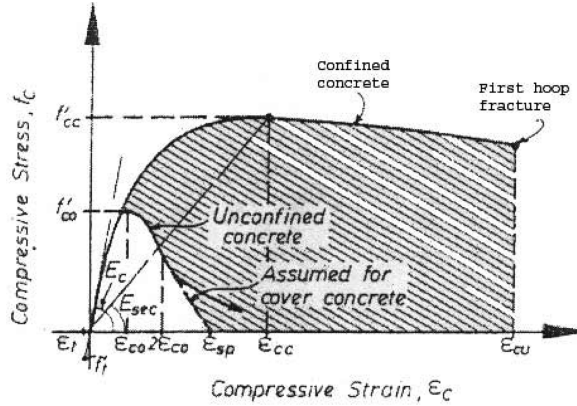


Fig. 1 Mander's stress-strain curve

They suggested a bilinear curve to model the response of FRP-confined concrete, in which intersection point of the lines corresponds to a strain of about 0.003 and the peak stress of the unconfined concrete, but they did not offered the model (Samaan *et al.* 1998).

In 1996, Rochette and Labossiere employed the multi-step FEM method to estimate the response of FRP-wrapped concrete columns. They modeled concrete as an absolute elastic-plastic material and admitted failure criterion of Druger-Pruger. However there was a good accordance between their models and experimental data, the model was not easy to use (Samaan *et al.* 1998).

Hoshikuma *et al.* (1997) presented a model for compressive stress-strain curve which has an increasing and decreasing part. (Hoshikuma *et al.* 1997) The relationship for increasing part is

$$f_c = E_c \varepsilon_{cc} \left[1 - \frac{1}{n} \left(\frac{\varepsilon_c}{\varepsilon_{cc}} \right)^{n-1} \right] \quad (12)$$

With

$$n = \frac{E_c \varepsilon_{cc}}{E_c \varepsilon_{cc} - f_{cc}} \quad (13)$$

Where E_c is elasticity module of the concrete; f_{cc} and ε_{cc} are peak stress and the corresponding strain in the reinforced concrete column which for circular sections are calculated through the relationships below

$$f_{cc} = f_{co}' \left(1 + 3.83 \frac{\rho_s f_{yh}}{f_{co}} \right) \quad (14)$$

$$\varepsilon_{cc} = 0.00218 + 0.0332 \frac{\rho_s f_{yh}}{f_{co}} \quad (15)$$

Where ρ_s is volumetric ratio of stirrups; f_{yh} is stirrup yield stress and f_{co} is compressive strength of the concrete.

Decreasing part of the compressive stress-strain model for circular columns of reinforced concrete was suggested as

$$f_c = f_{cc} - E_{des} (\varepsilon_c - \varepsilon_{cc}) \quad (16)$$

Where E_{des} is failure rate and it is obtained by regression of the experimental data in the range of ε_{cc} to ε_{cu} . Hoshikuma *et al.* (1997) suggested the relationship below to calculate E_{des}

$$E_{des} = 11.2 \frac{f_{co}^2}{\rho_s f_{yh}} \quad (17)$$

Definition of ε_{cu} is also a very important matter. The tests by Hoshikuma *et al.* (1997) showed that when the compressive stress is smaller than $0.5f_{cc}$ in the decreasing part, concrete core collapses and longitudinal rebars buckle. On this basis, the strain corresponding to $0.5f_{cc}$ in the decreasing part is suggested as ultimate compressive strain; therefore

$$\varepsilon_{cu} = \varepsilon_{cc} + \frac{f_{cc}}{2E_{des}} \quad (18)$$

In 1997, Monti and Spoelsra proposed a rather time consuming model which combines the model of stirrup confinement by Mander *et al.* (1998) with the relationships of volumetric strains by Pantazopoulou and Miller (1995) (Samaan *et al.* 1998).

In 1997, Mirmiran and Shahawy performed some tests on the tube-confined concrete specimens. They plotted lateral expansion ratio versus longitudinal strain. Lateral expansion ratio is the proportion of the lateral strain to the longitudinal strain. As the plot showed lateral expansion ratio increases up to a peak and then decreases until it reaches a constant value before the failure. They also concluded that confinement with an elastic-plastic material (like steel) affects the behavior of concrete very different from when an elastic material (like FRP) is used to confine (Mirmiran *et al.* 1997).

In 1997, Gao and Karbhari recommended two models for prediction of the ultimate axial stress and strain in composite-confined members with circular sections, one of which was obtained experimentally and the other one was basically an analytical model. Modeling of the ultimate behavior was based on the material properties (Karbhari and Gao 1997).

In 1998, Samaan *et al.* (1998) suggested a simple and accurate model based on the expansion properties of the FRP-confined concrete. In order to present a bilinear response for FRP-confined concrete, they employed the relationship by Richard and Abbot (1975) and then calibrated it as (Samaan *et al.* 1998)

$$f_c = \frac{f_c(E_1 - E_2)\varepsilon_c}{\left[1 + \left(\frac{(E_1 - E_2)\varepsilon_c}{f_o}\right)^n\right]^{\frac{1}{n}}} + E_2\varepsilon_c \quad (19)$$

Where ε_c and f_c is axial strain and stress of the confined concrete; E_1 , E_2 are primary and secondary slopes respectively; f_o is reference plastic stress (where the second slope intersect with stress axis) and n is controlling parameter of the transition part which depends on form of the curve. The model is not too sensitive to n and it is usually equal to 1.5.

If stress does not reach the maximum value of confined concrete, FRP does not have any confining effect. Hence, the primary slope of the stress-strain model depends solely on the concrete itself. Based upon this fact, the offered relationship for E_1 is affected only by compressive strength of the concrete. E_1 and E_2 are calculated according to the equations below

$$E_1 = 3950\sqrt{f'_c} \quad (20)$$

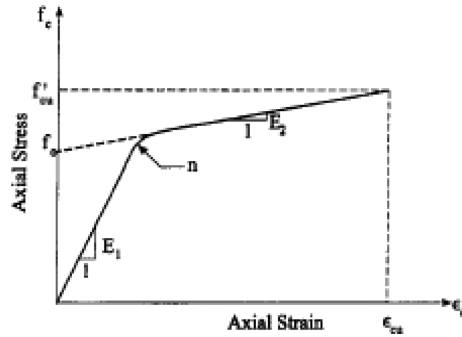


Fig. 2 Axial stress-strain model suggested by Samaan *et al.* (1998)

$$E_2 = 245.6f_c'^{0.2} + 1.3456\frac{E_j t_j}{D} \quad (21)$$

Where f' is strength of the unconfined concrete (MPa); E_j is effective elasticity module of the FRP tube in the tangent direction; t_j is tube thickness and D is column diameter.

f_o is a function of the unconfined concrete strength and confinement pressure applied by the FRP tube is calculated as

$$f_o = 9.872f_c' + 0.371f_r + 6.258 \quad (22)$$

Where f_r is confining pressure, with

$$f_r = \frac{2f_j t_j}{D} \quad (23)$$

Where f_j is tangent strength of the tube.

Samaan *et al.* (1998) estimated maximum stress and strain of the FRP tube-confined concrete as

$$f_{cu}' = f_c' + 6f_r^{0.7} \quad (24)$$

$$\epsilon_{cu} = \frac{f_{cu}' - f_o}{E_2} \quad (25)$$

In 1998, Mirmiran *et al.* (2000) studied effective parameters in the concrete confinement. The parameters were section shape, proportion of length to diameter and the bond of polymeric materials to concrete. The study showed that stress-strain curve is completely different for the distinct section shapes, thickening FRP jacket upgrades the ultimate strength of the cylinders considerably, but the rectangular sections are affected less in this respect, as a little change of ductility is observed in after the peak point. The researchers declared that distribution of confining pressure is responsible for the differences between the two sections. That is for cylindrical specimens pressure distribution is uniform and dependent on the ultimate radial strength of the tube, whereas in rectangular sections confining pressure is maximum at the corners and the small pressure between the corners depends on the moment rigidity of the tube (Mirmiran *et al.* 1997).

In 1999, Saafi *et al.* (1999) offered some explanations about the differences between confinement with steel and polymer fibers. The properties of confining materials make the confinements different. Before the failure, polymers have linear behavior, while on the contrary steel behaves

nonlinearly. In the case of poor confinement, FRP-confined concrete reaches maximum stress and strain simultaneously, but the steel-confined concrete loose strength when the steel yields. They found that the better bonding of the FRP jackets to concrete than the tubes (prefabricated FRP jackets) might be responsible for the different results of the two confinements. However, the studies by Mirmiran *et al.* (1998) showed that the bond between polymeric materials and concrete results in a little different behavior of the specimens (Saafi *et al.* 1999).

In 1999, Toutanji tested cylindrical specimens confined with different fibers (i.e., glass and carbon fibers). Ultimate compressive strength of the GFRP and CFRP confined cylinders increased 100% and 200% respectively. Failure mode of the wrapped cylinders was based on the jackets with sudden rupture (Toutanji 1999).

Suggested model of Toutanji (1999) is a bilinear curve which consists of two completely distinct equations. For the primary part, where confinement has a little effect due to insignificant expansion of the concrete core, stress-strain equation is

$$f_c = \frac{E_c \varepsilon_c}{1 + \left[\frac{E_c}{f_{ua}} - \frac{2}{\varepsilon_{cu}} + \frac{E_{ua} E_c \varepsilon_{cu}}{f_{ua}^2} \right] \varepsilon_c} \quad (26)$$

With

$$f_{ua} = f'_{co} \left[1 + 0.0178 \left(\frac{2E_{frp} t_{frp}}{f'_{co} D} \right)^{0.85} \right] \quad (27)$$

$$\varepsilon_{ua} = \varepsilon_{co} \left[1 + 0.0448 \left(\frac{2E_{frp} t_{frp}}{f'_{co} D} \right)^{0.85} \right] \quad (28)$$

$$E_{ua} = 0.3075 \frac{f'_{co}}{\varepsilon_{co}} \quad (29)$$

where ε_c is strain of the confined concrete; E_c is elasticity module of concrete; f'_{co} is unconfined concrete strength and D , t_{frp} , E_{frp} are FRP section diameter, thickness and elasticity module respectively.

The second part of the curve, where FRP is activated completely and concrete is affected by confinement, stress-strain curve obeys the equations below

$$f'_c = f'_{co} \left[1 + 3.5 \left(\frac{2E_{frp} t_{frp} \cdot \varepsilon_1}{f'_{co} D} \right)^{0.85} \right] \quad (30)$$

$$\varepsilon_c = \varepsilon_{co} \left[1 + (310.57 \varepsilon_1 + 1.9) \left(\frac{f'_c}{f'_{co}} - 1 \right) \right] \quad (31)$$

With $0.002 \leq \varepsilon_1 \leq \varepsilon_{frp,frp}$. Ultimate axial stress and strain is calculated by substituting the failure strain in the above equations.

It has always been important to study finite element model of confined concrete. For example Mirmiran *et al.* (2000) studied the FRP tube-confined concrete under pure axial load by using Ansys software (Mirmiran and Zagers 2000).

In 2000, Liu *et al.* examined performance of the bonding and fiber texture of dual composite jackets. Six-layer GFRP, AFRP and CFRP jackets were used with different texture degrees (45, 60 and 90) (Chaallal *et al.* 2003).

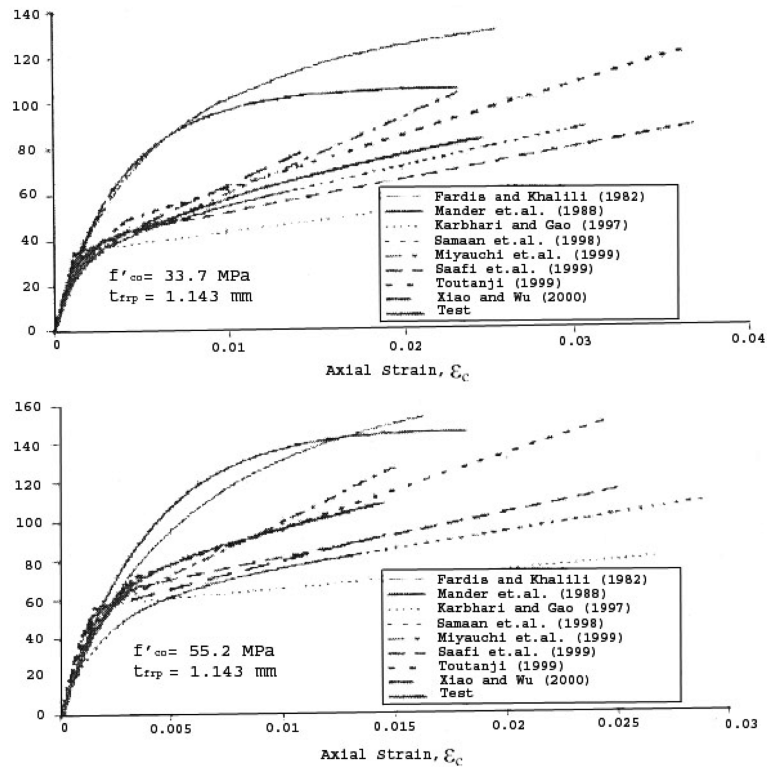


Fig. 3 Comparison of stress-strain curves suggested by different researchers (Fardis and Khalili 1981)

In 2002, Sheikh and Xiao tested reinforced concrete columns under constant axial load and lateral seismic loads (to simulate the loads applied by an earthquake). The results showed that FRP composite with carbon and glass fibers could effectively upgrade the strength of weak columns to such an extent that under seismic loading, strengthened columns behaves like or better than the columns designed by ACI 318-99. Besides, FRP composite increases strength, ductility and energy absorbing capacity of reinforced concrete columns significantly (Li and Sung 2004).

In 2001, Fam and Rizkalla applied pure moment to the specimens with circular sections. FRP and steel tube were selected to cast the concrete in them. It was resulted that bending behavior strictly depends on rigidity and ratio of diameter to thickness of the tube and also, confinement has nearly no important effect on moment strength (Fam and Rizkalla 2001).

In 2003, Chaallal *et al.* (2003) suggested a model for rectangular sections confined by composites, which was the first 3-line model for confined concrete. Their model depends on the axial rigidity of the concrete and lateral rigidity of the jacket (Chaallal *et al.* 2003).

In 2004, Li and Sung proposed a model (called modified L-L model) while they were studying shear failure of the circular piers confined by FRP jackets. Then, they applied this model to confinement of the piers by CFRP and analyze of the lateral force-displacement circular columns (Li and Sung 2004).

In 2006, Perera offered a simplified model of damage (based on the continuous damage mechanics) for evaluation and resistant design of the columns under skew bending (Perera 2006).

2.2 Theoretical background

Many researches proposed models for the behavior of reinforced concrete columns against cyclic loads (Li *et al.* 2003). This behavior depends on parameters of the concrete column like amount of the axial load, confinement, shear strength, flexural strength, concrete material and some other parameters. One of the important parameters is the amount of confinement. In the unstrengthened concrete columns, the transverse reinforcing can produce the confinement for concrete. The shape of the reinforcing can affect the amount of the confinement of columns. For example Wakabayashi (Wakabayashi 1986) presented the difference between types of reinforcing in columns and their effects in hysteresis curves. In this research the numerical analysis for the strengthened columns has been presented and finally the simplified models for strengthened reinforce columns have been proposed using numerical modeling.

3. Description of samples and modeling

3.1 Modeling method

In order to study the structural behavior, two methods are available. The first method is to model the elements experimentally and the second one is the finite element modeling by means of the related computer software. Experimental method is usually difficult, especially when a high number of specimens are needed to study the effects of different agents. Hence, finite element modeling is selected in this paper and Ansys 11 computer software is employed to study nonlinear behavior of the structures.

Ansys 11 supports a high variety of elements and nonlinear properties of the materials could be defined properly in this software. Ansys 11 is able to run static, time history, modal, spectrum and thermal analyses so that it can handle many engineering problems.

3.2 Material properties

3.2.1 Concrete properties

Elastic properties of the concrete are defined as $E=2.1 \times 10^4$ MPa and $\nu=0.17$. Then in Ansys, concrete is selected from the nonlinear inelastic materials, which is the best definition for describing the nonlinear properties of concrete. For modeling nonlinear behavior of the concrete, Ansys requires compressive and tensile strength, shear transfer coefficient for open and closed cracks, etc. Compressive and tensile strengths are defined as 24 MPa and 2.5 MPa. Shear transfer coefficient is equal to zero for smooth cracks (i.e., no shear transition) and one for rough cracks (i.e., full shear transition).

3.2.2 Steel properties

Elastic properties of steel are supposed to be $E=210$ GPa and $\nu=0.3$. Nonlinear behavior of steel is modeled by a stress-strain model, in which yield stress is $F_y=400$ MPa for rebars (Fig. 4) and $F_y=240$ MPa for steel casing.

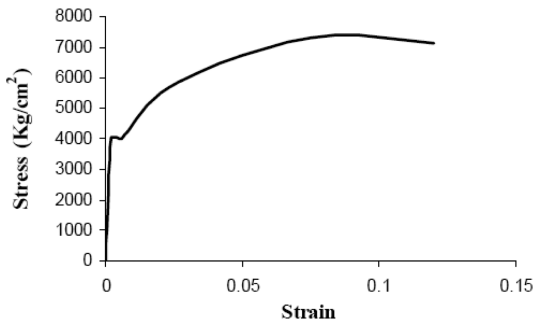


Fig. 4 Stress-strain curve for rebars

Table 1 CFRP properties

120E3 MPA	Elasticity module in fiber direction
1.5E3 MPA	Tensile strength in fiber direction
0.35 mm	Layer thickness
0.018	Ultimate Strain

3.2.3 FRP properties

Properties of the FRP jackets are available in Table 1.

3.3 Elements

3.3.1 SOLID65 (3D reinforce concrete element)

This element is used to model concrete, reinforced composites (like fiberglass) and geotechnical materials. It could be cracked in all three perpendicular directions and collapse, plastic deformation and creep can be considered for it (Fig. 5).

3.3.2 LINK8

It is a 3D bar element defined by two end nodes, section area and initial strain. The element is applied for trusses, cables, links, springs, etc. and it can bear both tension and compression. Each end node has three degree of freedom (X , Y and Z displacement). No moment is considered in the nodes due to the hinging property of them. In the current study LINK8 is selected to model longitudinal and transverse reinforcements (Fig. 6).

3.3.3 SOLID46 (for FRP modeling)

This element is used to model multilayer shells. The element could have up to 250 layers and it has three degree of freedom (X , Y and Z displacement) in each node. SOLID46 is defined by 8

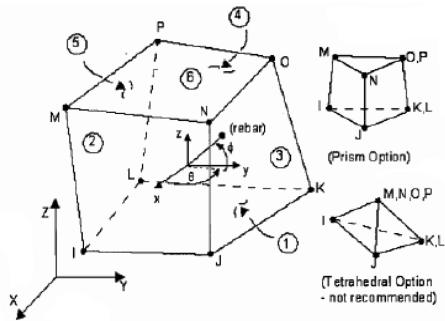


Fig. 5 SOLID65 element

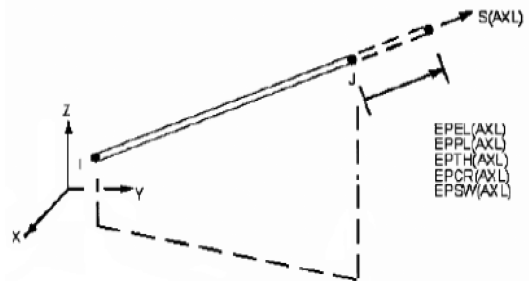


Fig. 6 LINK8 element

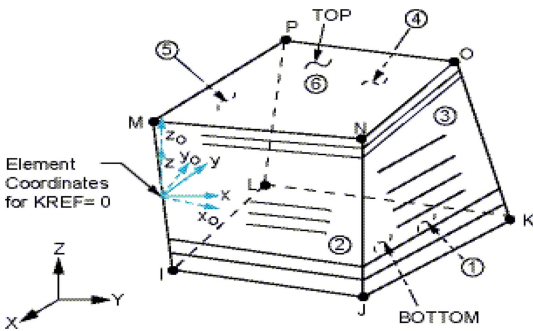


Fig. 7 SOLID46 element

Table 2 Geometric details of models

Height of columns	3 m
Diameter	0.7 m
Concrete cover thickness	0.025 m
Transverse reinforcement	Φ10@0.15 m

nodes, thickness and angle of the layers and orthotropic properties of the materials (Fig. 7). Tsai-Wu criterion is selected for the failure of FRP.

3.4 Description of specimens

All models have similar geometrics properties. They are circular with diameter of 0.7 m and height of 3 m. These properties have been shown in Table 2. Thicknesses of CFRP in all models are similar (0.3 mm), and all of the models have transverse reinforcement in shape of Φ10@0.15 m in whole length of the models.

In this research it is supposed that the confinement of the columns is less than requirements and they need to be strengthened using FRP layers. Because of this assumption, all models have same transverse reinforcing which is not enough for confinement of all of them, but it is enough for enduring the applied shear strength to prevent generating shear hinges.

3.5 Loading

The modeled pier is fixed at the end, i.e., no freedom degree exists (neither displacement nor rotation). To apply load on the pier, a vertical load is considered as dead load, which is distributed compressively on the upper nodes. Besides, a displacement load is applied at the pier's end to

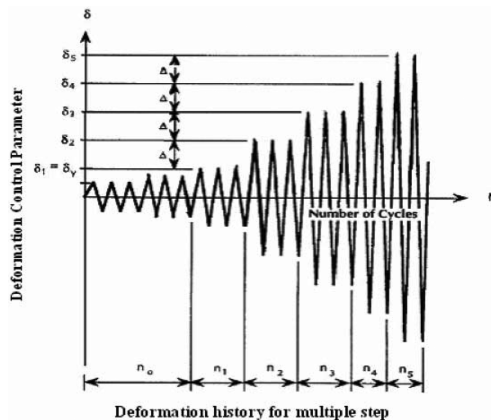


Fig. 8 Cyclic loading

consider drift of the member under seismic loads. Two displacement loads are specified:

Static displacement load, applied as a unidirectional load at the top of pier. Increasing cyclic displacement load, selected according to suggested loading of experimental tests, which is used in many references to study the behavior of concrete piers (Fig. 8). In this loading displacement increases by Δ in each step, which in the current study it is supposed that $\Delta = \delta Y / 2$. Displacement loading is continued until $\mu = \pm 3.5$, with $\mu = \delta / \delta Y$. Hysteresis curves of the next sections are base shear-drift curves obtained by this loading.

4. Methodology

Parameters of the plastic hinges are evaluated in three steps. After performing these three steps, results of all models have been shown in a table. Steps is presented below.

4.1 Plotting hysteresis curves

Models are analyzed in Ansys 11 and hysteresis curves (force-displacement and moment-rotation) are obtained for them (FEMA 440 2005) (Fig. 9).

4.2 Plotting envelope curves

When the hysteresis curves are obtained, envelope curves are drawn based on the instructions in FEMA 440 (Fig. 10).

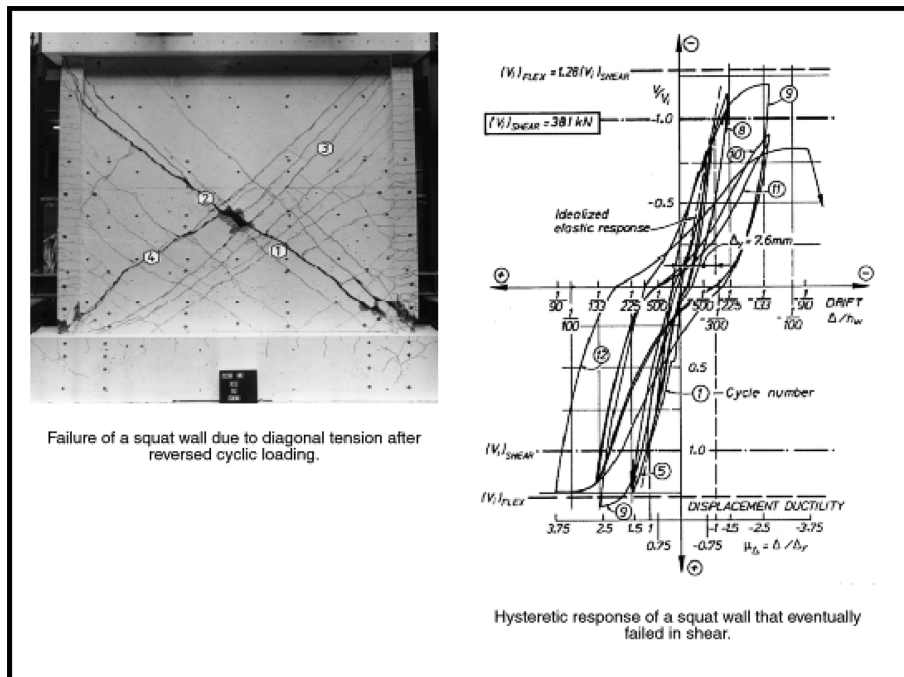


Fig. 9 Hysteresis curve (FEMA 440 2005)

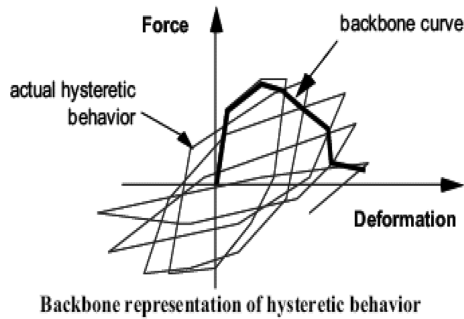


Fig. 10 Plotting envelope curve (FEMA 440 2005)

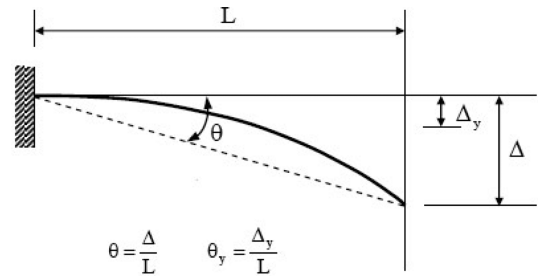


Fig. 11 Definition of rotation (FEMA 2000)

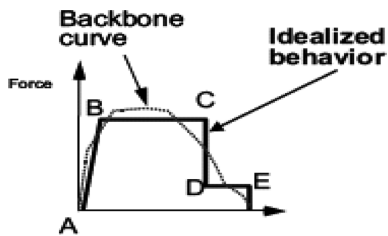


Fig. 12 Idealization of envelope curve (FEMA 440 2005)

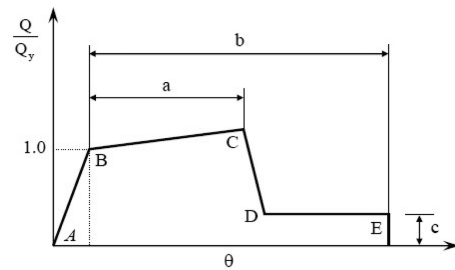


Fig. 13 General plot of load-deformation curve for concrete members (FEMA 2000)

4.3 Idealization of envelope curves

In static nonlinear analysis, it is possible to show plastic hinge properties with three parameters (a , b and c). As Fig. 11 shows, rotation of the pier comprises both elastic and plastic rotations. Fig. 12 displays the envelope of nonlinear load-deformation and idealization of it.

5. Results and discussion

As already stated, the aim of this paper is determination of required parameters for plastic hinges in static nonlinear analysis of the FRP-wrapped columns. After nonlinear analysis of the models in Ansys 11, obtained hysteresis, envelope and idealized curves are displayed in this section for comparison. At the end, a table of evaluated parameters is offered for plastic hinges of FRP-wrapped columns, which could be employed for nonlinear static analysis.

Three plots are observed for each model: force-displacement, moment-rotation and envelope curve which is provided by an idealized curve. The first model belongs to a column without FRP (Fig. 14). As the hysteresis force-displacement plot shows, the curve descends gradually after it reaches 180 kN, i.e., rigidity of the elements decreases until the model fails in the lateral displacement of 48 mm. Envelope curve of the moment-rotation hysteresis curve is observed in Fig. 14c and the parameters a , b and c are obtained by using the instruction for seismic rehabilitation (Fig. 13). As the figure indicates, the results of analysis agree with the mentioned instruction for the concrete columns. Fig. 15 represents a FRP-wrapped concrete column, in

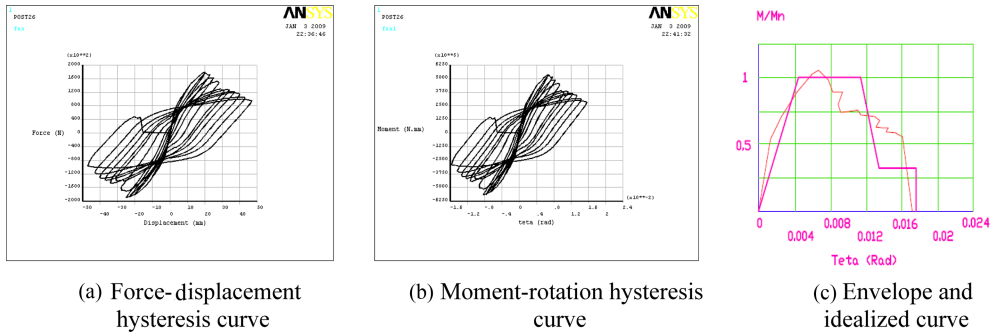


Fig. 14 The model without FRP

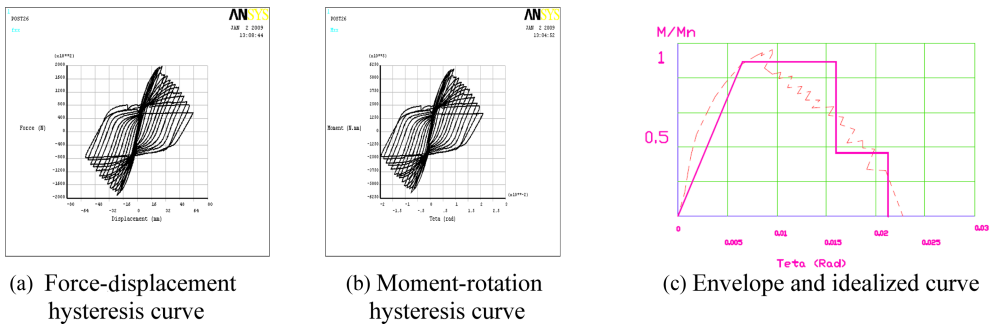


Fig. 15 Model 1

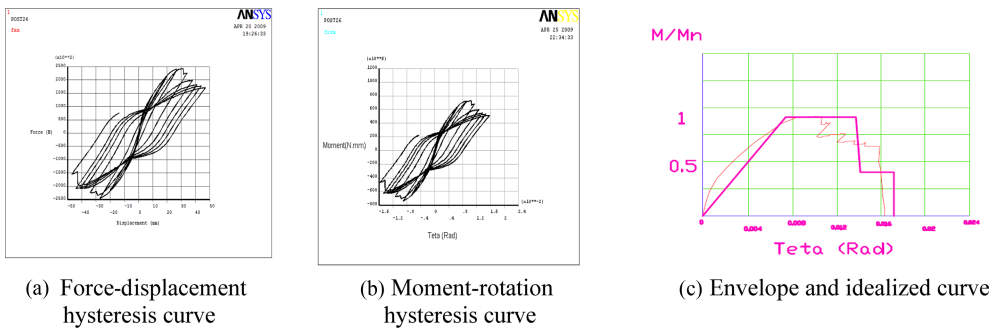


Fig. 16 Model 2

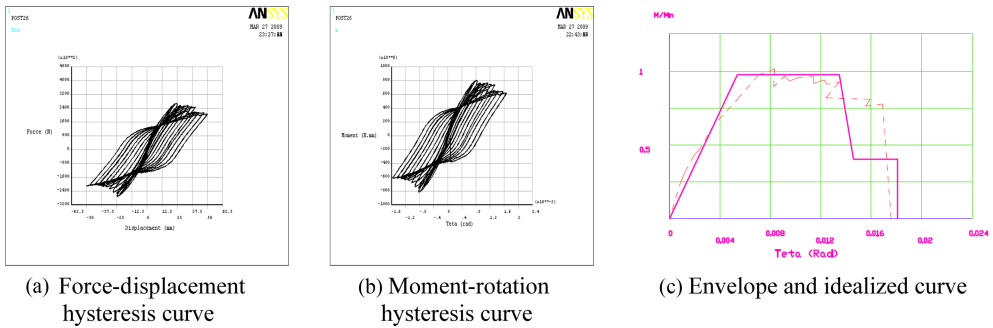
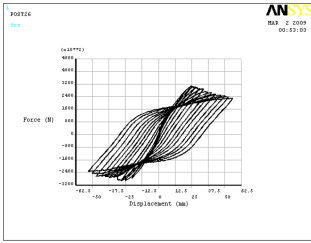
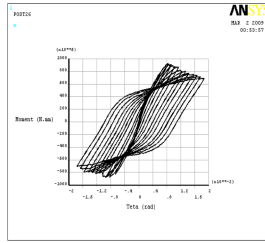


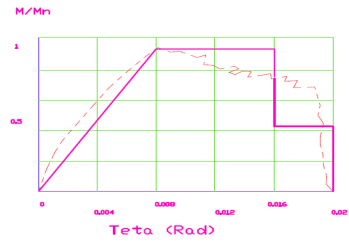
Fig. 17 Model 3



(a) Force-displacement hysteresis curve

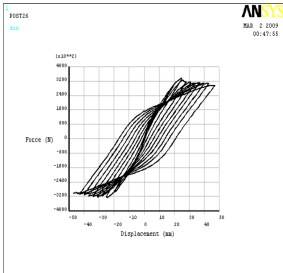


(b) Moment-rotation hysteresis curve

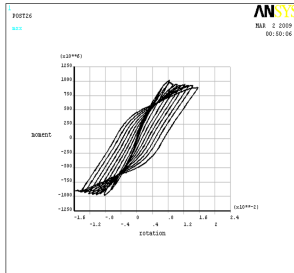


(c) Envelope and idealized curve

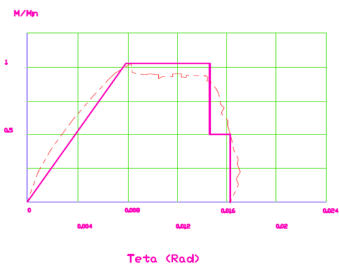
Fig. 18 Model 4



(a) Force-displacement hysteresis curve

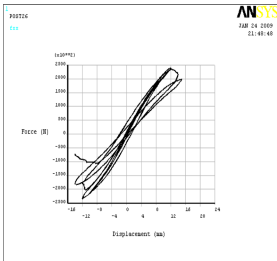


(b) Moment-rotation hysteresis curve

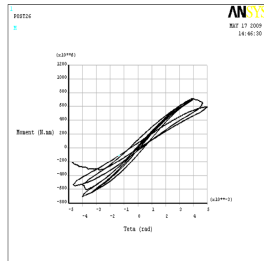


(c) Envelope and idealized curve

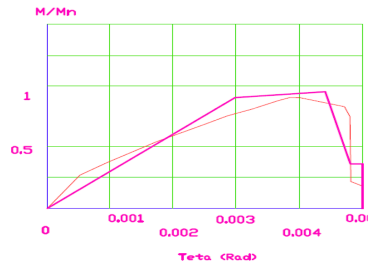
Fig. 19 Model 5



(a) Force-displacement hysteresis curve

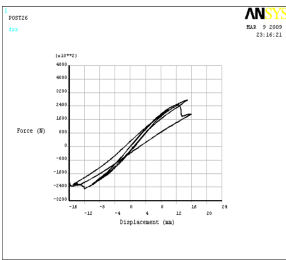


(b) Moment-rotation hysteresis curve

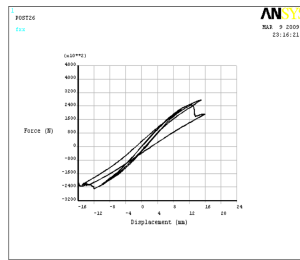


(c) Envelope and idealized curve

Fig. 20 Model 6



(a) Force-displacement hysteresis curve

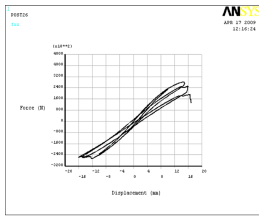


(b) Moment-rotation hysteresis curve

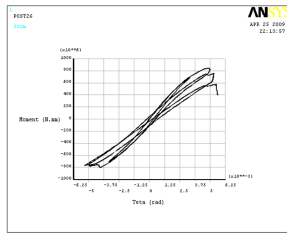


(c) Envelope and idealized curve

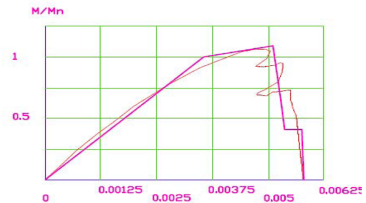
Fig. 21 Model 7



(a) Force-displacement hysteresis curve

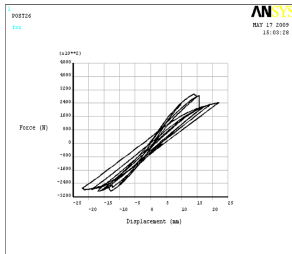


(b) Moment-rotation hysteresis curve

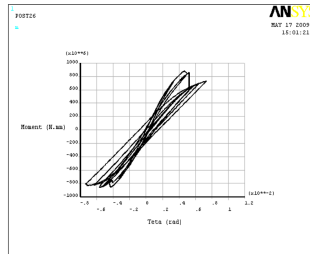


(c) Envelope and idealized curve

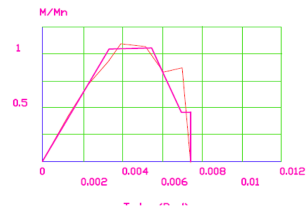
Fig. 22 Model 8



(a) Force-displacement hysteresis curve

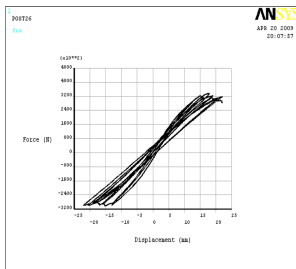


(b) Moment-rotation hysteresis curve

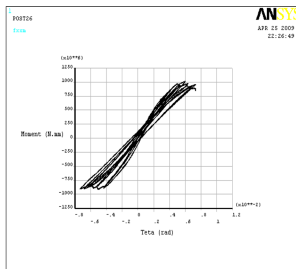


(c) Envelope and idealized curve

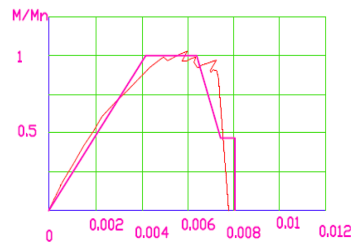
Fig. 23 Model 9



(a) Force-displacement hysteresis curve

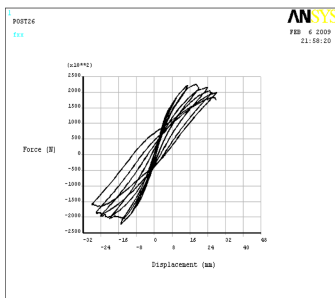


(b) Moment-rotation hysteresis curve

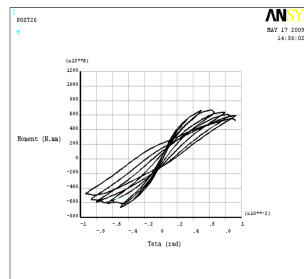


(c) Envelope and idealized curve

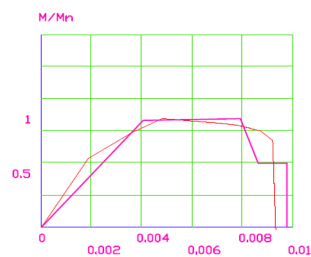
Fig. 24 Model 10



(a) Force-displacement hysteresis curve

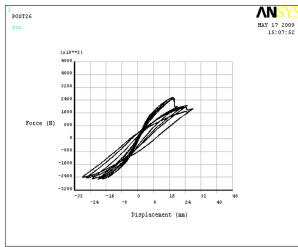


(b) Moment-rotation hysteresis curve

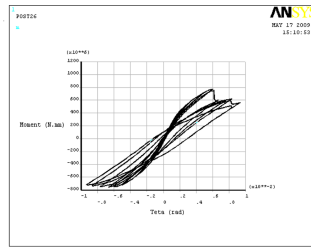


(c) Envelope and idealized curve

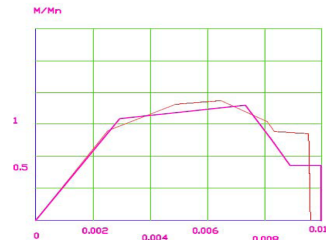
Fig. 25 Model 11



(a) Force-displacement hysteresis curve

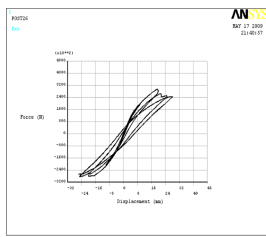


(b) Moment-rotation hysteresis curve

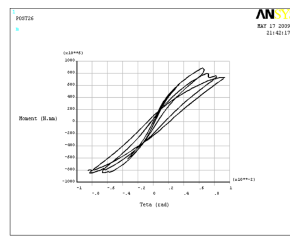


(c) Envelope and idealized curve

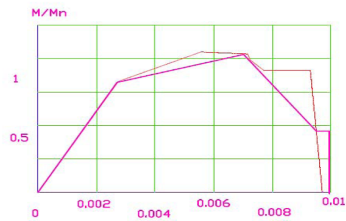
Fig. 26 Model 12



(a) Force-displacement hysteresis curve

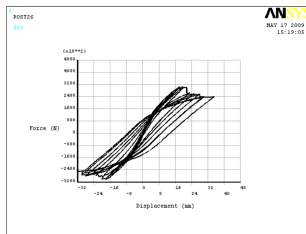


(b) Moment-rotation hysteresis curve

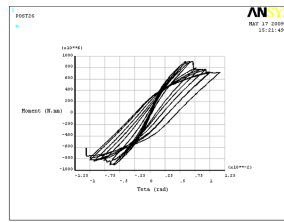


(c) Envelope and idealized curve

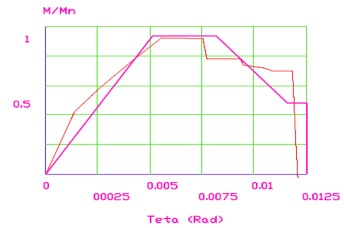
Fig. 27 Model 13



(a) Force-displacement hysteresis curve

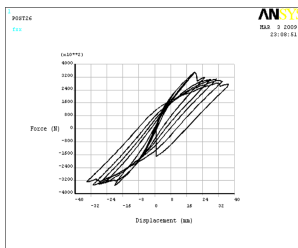


(b) Moment-rotation hysteresis curve

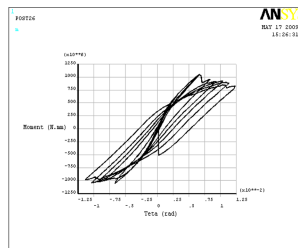


(c) Envelope and idealized curve

Fig. 28 Model 14



(a) Force-displacement hysteresis curve



(b) Moment-rotation hysteresis curve



(c) Envelope and idealized curve

Fig. 29 Model 15

which the maximum force increases from 180 kN to 200 kN. Moreover, maximum displacement increases considerably, which implies the increase of ductility due to the confinement. The envelope and the idealized curve in Fig. 15c show an increase of the parameters a , b and c .

6. Conclusions

After performing all analysis, using above results (Figs. 14-29), the specifications of the plastic hinges can be obtained. Plastic hinge properties vary with the FRP wrapped around the piers (Table 4). The amount of parameters a , b and c can be used in defining plastic hinge properties in pushover analysis of the columns which strengthened by FRP.

As it is shown in the Table 4, the plastic hinge parameters increase for the FRP-wrapped piers. That is the rehabilitation of piers upgrades their ductility. In the FRP-wrapped piers, plastic hinge parameters decrease as the axial load increases; i.e., the failure of member becomes more brittle. Also increase of rigidity decreases the deformation. For the same loading, strengthened piers deform less than the unstrengthened ones and as it was anticipated, wrapping piers with FRP increases ductility and energy absorbing capacity of them. By using the above table concentrated hinges can be defined in any macro model for decreasing the time of analysis.

Table 4 Plastic hinge parameters

FRP layer properties	Model No.	Axial compression (MPa)	Areal ratio of the longitudinal rebars	Parameters		
				a	b	c
No FRP	0	2.5	0.01	0.006	0.015	0.2
	1	2.5	0.01	0.011	0.017	0.35
	2	2.5	0.015	0.009	0.014	0.35
	3	2.5	0.02	0.008	0.012	0.36
	4	2.5	0.025	0.004	0.01	0.4
	5	2.5	0.03	0.006	0.009	0.4
	6	10	0.01	0.0015	0.002	0.34
	7	10	0.015	0.0018	0.0024	0.37
	8	10	0.02	0.0014	0.0019	0.37
	9	10	0.025	0.001	0.0026	0.38
	10	10	0.03	0.002	0.003	0.38
	11	6.25	0.01	0.004	0.005	0.42
	12	6.25	0.015	0.003	0.0046	0.39
	13	6.25	0.02	0.004	0.0055	0.4
	14	6.25	0.025	0.0045	0.0065	0.4
15	6.25	0.03	0.0043	0.006	0.38	

References

- AASHTO (2002), *Standard specification for highway bridges*, 17th Edition, American Association of State Highway and Transportation Officials, Washington D.C.
- ANSYS Standard Users Manual Help, Ver.11 and ANSYS Structural Nonlinearities Manual.
- ACI Committee 440 (1996), *State-of-the-art report on FRP for concrete structures (ACI 440R-96)*, Manual of Concrete Practice, American Concrete Institute, Farmington with Hills, Michigan, 68.
- ACI Committee 440 (2000), *Guide for the design and construction of externally bounded FRP systems for strengthening concrete structures*, ACI Code, Reported by ACI Committee 440.
- ATC40 (1997), *Seismic evaluation and retrofit of concrete buildings*.
- Bank, L.C. (2006), *Composites for construction, structural design with FRP materials*, John Wiley and Sons Inc, Hoboken, New Jersey, Canada.
- Challal, O., Hassan, M. and Shahawy, M. (2003), "Confinement model for axially loaded short rectangular columns strengthened with fiber reinforced polymer wrapping", *ACI Struct. J.*, **100**(2), 215-221.
- Chen, W.F. (1994), *Constitutive equations for engineering materials*, Elsevier Science, **2**(1), 1096.
- Fam, A.Z. and Rizkalla, S.H. (2001), "Confinement model for axially loaded concrete confined by circular fiber reinforced polymer tubes", *ACI Struct. J.*, **98**(4), 451-461.
- Fardis, M.N. and Khalili, H. (1981), "Concrete encased in fiberglass reinforced plastic", *ACI J.*, **76**(6), 440-446.
- FEMA 356 (2000), *NEHRP Recommended provisions for the seismic rehabilitation of buildings*.
- FEMA 440 (2005), *NEHRP Recommended provisions for the improvement of nonlinear static seismic analysis procedures*.
- FHWA (1995), *Seismic retrofit manual for highway bridges*, Publication No. FHWA/RD-052, McLean, VA.
- Hoshikuma, J., Kawashima, K., Nagaya, K. and Taylor, W. (1997), "Stress-strain model for confined reinforced concrete in bridge piers", *J. Struct. Eng.-ASCE*, **123**(5), 624-633.
- Inel, M. and Ozmen, H.B. (2006), "Effect of plastic hinge properties in nonlinear analysis of reinforced concrete buildings", *Eng. Struct.*, **28**(11), 1494-1502.
- Karbhari, V.M. and Gao, Y. (1997), "Composite jacketed concrete under uniaxial compression _Verification of simple design equations", *J. Mater. Civil Eng.*, **9**(4), 185-193.
- Lee, J. and Fenves, G.L. (1998), "Plastic-damage model for cyclic loading of concrete structures", *J. Eng. Mech.*, **124**(8), 892-900.
- Li, Y.F., Lin, C.T. and Sung, Y.Y. (2003), "A constitutive model for concrete confined with carbon fiber reinforced plastics", *Mech. Mater.*, **35**(3-6), 603-619.
- Li, Y.F. and Fang, T.S. (2004), "A constitutive model for concrete confined by steel reinforcement and carbon fiber reinforced plastic sheet", *Struct. Eng. Mech.*, **18**(1), 21-40.
- Li, Y.F. and Sung, Y.Y. (2004), "A study on the shear-failure of circular sectioned bridge column retrofitted by using CFRP jacketing", *J. Reinf. Plast. Comp.*, **23**(8), 811-830.
- Mander, J.B., Priestley, M.J.N. and Park, R. (1988), "Theoretical stress-strain model for confined concrete", *J. Struct. Eng.-ASCE*, **114**(8), 1804-1826.
- Mirmiran, A., Zagers, K. and Yuan, W. (2000), "Nonlinear finite element modeling of concrete confined by fiber composites", *Finite Elem. Anal. Des.*, **35**(1), 79-96.
- Mirmiran, A. and Shahawy, M. (1997), "Behavior of concrete columns confined by fiber composites", *J. Struct. Eng.-ASCE*, **123**(5), 583-590.
- Perera, R. (2006), "A numerical model to study the seismic retrofit of RC columns with advances Composite Jacketing", *Compos. Part B-Eng.*, **37**(4-5), 337-345.
- Saatcioglu, M. and Razvi, S. (1992), "Strength and ductility of confined concrete", *J. Struct. Div.-ASCE*, **118**(6), 1590-1607.
- Saafi, M., Toutanji, H. and Li, Z. (1999), "Behavior of concrete columns confined with reinforced polymer tubes", *ACI Mater. J.*, **96**(4), 500-509.
- Samaan, M., Mirmiran, A. and Shahawy, M. (1998), "Model of concrete confined by fiber composites", *J. Struct. Eng.-ASCE*, **124**(9), 1025-1031.
- Sarrazin, J. (2004), *A Comparative analysis of seismic retrofit techniques for reinforced concrete bridge columns*, PHD Thesis, University of Ottawa, Canada.

- Shahawy, M., Mirmiran, A. and Beitelman, T. (2000), "Tests and modeling of carbon wrapped concrete columns", *Compos. Part B.-Eng.*, **31**(6-7), 471-480.
- Sheikh, S.A. and Uzumeri, S.M. (1980), "Analytical model for concrete confinement in tied columns", *J. Struct. Div.-ASCE*, **108**(12), 2073-2722.
- Syngros, C., Mylonakis, G and Gazetas, G (2004), "Geotechnical effects in the collapse of Fukae (Hanshin Expressway) Bridge, Kobe, 1995", Yegian, M.K., and Kavazanjian, E., - Editors, July 27-31, 2004 Los Angeles, California, USA, Geotechnical Engineering for Transportation Projects (GPS No. 126) 2004 ASC.
- Toutanji, H. (1999), "Stress-strain characteristics of concrete columns externally confined with advances fiber Composite sheets", *ACI Mater. J.*, **96**(3), 397-404.
- Vistaps, M. Karbhari (2004), "Fiber reinforced composite bridge system – transition from the laboratory to the field", *Compos. Struct.*, **66**(1-4), 5-16.
- Wakabayashi, M. (1986), *Design of earthquake-resistant buildings*, McGraw Hill: New York.
- Xiao, Y. and Wu, H. (2000), "Compressive behavior of concrete confined by carbon fiber Composite jackets", *J. Mater. Civil Eng.*, **12**(2), 139-146.
- Youssef, M.N. (2003), *Stress-strain model for concrete confined by FRP composites*, PHD Thesis, University of California, Irvine.

NB